# Semiconducting Diblock Copolymers Synthesized by Means of Controlled Radical Polymerization Techniques

**Ulf Stalmach, Bert de Boer, Christine Videlot, Paul F. van Hutten, and Georges Hadziioannou***

*Contribution from the Department of Polymer Chemistry and Materials Science Centre, University of Groningen, Nijenborgh 4, NL-9747 AG Groningen, The Netherlands*

*Received January 14, 2000*

**Abstract:** A donor−acceptor, rod−coil diblock copolymer has been synthesized with the objective of enhancing the photovoltaic efficiency of the PPV−$C_{60}$ (PPV = poly(*p*-phenylenevinylene)) system by the incorporation of both components in a molecular architecture that is self-structuring through microphase separation. Diblock copolymers were obtained by using an end-functionalized rigid-rod block of poly(2,5-dioctyloxy-1,4-phenylenevinylene) as a macroinitiator for the nitroxide-mediated controlled radical polymerization of a flexible poly(styrene-*stat*-chloromethylstyrene) block. The latter block was subsequently functionalized with $C_{60}$ through atom-transfer radical addition. In a spin-cast film of the final diblock copolymer, the luminescence from PPV is strongly quenched, indicating efficient electron transfer to $C_{60}$. Under suitable conditions, solution-cast films of these diblock copolymers exhibit micrometer-scale, honeycomb-like patterns of holes.

## Introduction

In recent years, the demand for advanced organic materials with new properties has sparked the development of novel and innovative synthetic methods that allow one to implement the desired functionality in a predictable and controllable way. Since many of these functional materials are of a composite nature, some structural organization is usually required for the material to efficiently perform its function. The organization may vary, from simple dispersion with a proper domain size to preferential alignment, periodicity, asymmetry, etc. For the creation of the necessary structural order, with structural elements covering a wide range of length scales, concepts from supramolecular organic chemistry have been applied with great success.[1−3] Meanwhile, the now classical phenomenon of microphase separation in block copolymers[4−6] may also be exploited to realize self-structuring.[7,8] The chemical connectivity between the blocks forces the self-structuring to be on the same scale as the radius of gyration of the macromolecules, i.e., on a scale of 10−50 nm. For the simplest case, that of fully flexible (coil−coil), noncrystallizing diblock copolymers, phase separation sets in when $\chi N$ exceeds a critical value; $\chi$ represents the interaction enthalpy and $N$ the degree of polymerization (entropy factor). A set of semicontinuous and cocontinuous two-phase morphologies has been identified. The stability limits of these morphologies depend primarily on the block length ratio. Actual structures obtained may not represent thermodynamic equilibrium and will depend on the phase separation mechanism (spinodal decomposition or nucleation and growth) and on kinetic factors of mass transport. The phase diagram is different for rod−coil block copolymers,[9,10] or when crystallization is involved. Only limited knowledge has been gathered about these more complicated systems, so far. Similarly, the more involved and diverse morphologies found for triblock copolymers remain largely unexplored (see, e.g., ref 11).

A prime example of a multicomponent material that could benefit from morphological structuring is the active layer of a photovoltaic cell. In such a device, the active thin film is a composite of electron-donor molecules and electron-acceptor molecules, between dissimilar electrodes (for instance, Al and indium−tin oxide). In the accepted scenario, the excitation of a donor molecule by light is followed by electron transfer to the acceptor (exciton dissociation), after which separation and transport of the opposite charges, hole and electron, take place under the influence of the built-in electric field caused by the asymmetric electrode contacts.[12,13] The performance of this type of device is very sensitive to the morphology of the active layer. Obviously, both the donor and the acceptor phases should form a continuous path to their electrode to allow bipolar charge transport. Ideally, to ensure efficient exciton dissociation, an acceptor species should be within the exciton diffusion range

* Corresponding author. Phone: +31 50 3634300. Fax: +31 50 3634400. E-mail: hadzii@chem.rug.nl.

(1) Goodby, J. W.; Mehl, G. H.; Saez, I. M.; Tuffin, R. P.; Mackenzie, G.; Auzély-Velty, R.; Benvegnu, T.; Plusquellec, D. *Chem. Commun.* **1998**, 2057−2070.

(2) Ruokolainen, J.; Mäkinen, R.; Torkkeli, M.; Mäkelä, T.; Serimaa, R.; ten Brinke, G.; Ikkala, O. *Science* **1998**, *280*, 557−560.

(3) Bosman, A. W.; Janssen, H. M.; Meijer, E. W. *Chem. Rev.* **1999**, *99*, 1665−1688.

(4) Helfand, E.; Wasserman, Z. R. In *Developments in Block Copolymers-1*; Goodman, I., Ed.; Applied Science Publishers: New York, 1982; Chapter 4.

(5) Bates, F. S.; Fredrickson, G. H. *Annu. Rev. Phys. Chem.* **1990**, *41*, 525−557.

(6) Bates, F. S. *Science* **1991**, *251*, 898−905.

(7) Lodge, T. P.; Muthukumar, M. *J. Phys. Chem.* **1996**, *100*, 13275−13292.

(8) Stupp, S. I.; LeBonheur, V.; Walker, K.; Li, L. S.; Huggins, K. E.; Keser, M.; Amstutz, A. *Science* **1997**, *276*, 384−389.

(9) Matsen, M. W.; Barrett, C. *J. Chem. Phys.* **1998**, *109*, 4108−4118.

(10) Lee, M.; Cho, B.-K.; Kang, Y.-S.; Zin, W.-C. *Macromolecules* **1999**, *32*, 7688−7691.

(11) Breiner, U.; Krappe, U.; Thomas, E. L.; Stadler, R. *Macromolecules* **1998**, *31*, 135−141.

(12) Yu, G.; Pakbaz, K.; Heeger, A. J. *Appl. Phys. Lett.* **1994**, *64*, 3422−3424.

(13) Yu, G.; Gao, J.; Hummelen, J. C.; Wudl, F.; Heeger, A. J. *Science* **1995**, *270*, 1789−1791.

10.1021/ja000160a CCC: $19.00 
Published on Web 05/27/2000

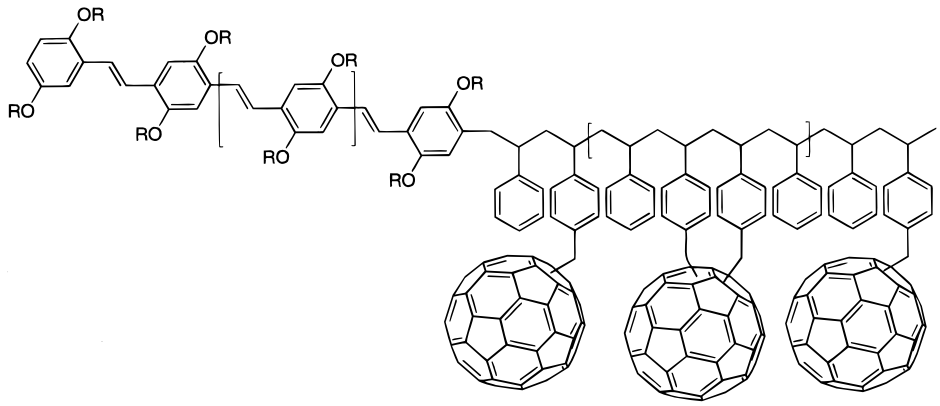


**Figure 1.** General structure of the target compounds.

from any donor species, and vice versa. Since the exciton diffusion range is typically several nanometers, and therefore shorter than the light absorption depth (~100 nm), the convoluted donor−acceptor interface of an interpenetrating morphology[13,14] should be more efficient in terms of exciton dissociation than a planar double-layer structure. In the optimized morphology, the characteristic size of the channels of the phases is matched to the exciton diffusion range. In principle, structuring on this scale may be achieved through phase separation in diblock copolymer films. In the particular case of a photovoltaic material, this requires the availability of a copolymer of suitable donor and acceptor blocks.

Conjugated molecules and polymers have emerged as new materials for optoelectronic applications during the 1990s.[15] For photovoltaic cells, the combination of a *p*-phenylenevinylene-type polymer (PPV) or oligomer as the donor material with $C_{60}$ as the acceptor has proven promising.[16−18] *p*-Phenylenevinylene-based materials are widely investigated for their optoelectronic properties[19−22] and their commercial application in light-emitting displays has arrived recently. While these materials are fairly good hole conductors, electron transport is poorer, which limits the performance in applications in which PPV is the sole active component, because of the resulting unbalanced charge transport. This problem is alleviated in the two-component, two-phase concept for photovoltaic devices outlined above, in which the acceptor transports the electrons. The ability of $C_{60}$ to accept several electrons[23] makes it a particularly attractive material for this purpose. Its low solubility is a major drawback, however. A way to overcome this is the incorporation of $C_{60}$ into polymers, thus yielding materials that combine the physical properties of fullerene with the processability of polymers.[24,25] Different approaches taken so far comprise, for example, radical copolymerization,[26] anionic grafting,[27] or polycycloaddition[28] with bare $C_{60}$, or the use of functionalized fullerenes.[29−31] Examples of the incorporation into preformed polymers include addition reactions of $C_{60}$ with amines,[32] azides,[33] or radicals created from alkoxyamines.[34]

According to the principles laid out above, a self-structuring photovoltaic composite may be formed from a diblock copolymer consisting of a PPV block and a block densely functionalized with $C_{60}$ (Figure 1). For the formation of block copolymers, a large array of synthetic strategies is available to the chemist. The most prominent of these is living anionic polymerization.[35] This method yields products with very low polydispersities, but it has its drawbacks. One is the necessity to work under very strict conditions to avoid impurities such as water and oxygen. Moreover, the highly reactive carbanion prohibits the use of various functional groups.[36] Recently, this has been overcome to some extent by the development of the controlled/"living" radical polymerization techniques[37] using either stable nitroxide counter radicals[38,39] (nitroxide-mediated "living" radical polymerization, NMRP) or atom-transfer radical polymerization (ATRP).[40] Both these techniques employ the principle of an equilibrium between a low concentration of active radicals and a rather large number of dormant species. This suppresses bimolecular side reactions such as recombination or disproportionation to such a degree that the overall polymerization process shows living characteristics, e.g., the increase of the molecular weight with conversion and the possibility to synthesize block copolymers.

(14) Halls, J. J. M.; Walsh, C. A.; Greenham, N. C.; Marseglia, E. A.; Friend, R. H.; Moratti, S. C.; Holmes, A. B. *Nature* **1995**, *376*, 498−500.
(15) *Handbook of Organic Conductive Molecules and Polymers*, Nalwa, H. S., Ed.; John Wiley & Sons: New York, 1997; Vols. 1−4.
(16) Sariciftci, N. S.; Smilowitz, L.; Heeger, A. J.; Wudl, F. *Science* **1992**, *258*, 1474−1476.
(17) Brabec, C. J.; Sariciftci, N. S. In *Semiconducting Polymers—Chemistry, Physics and Engineering*; Hadziioannou, G., van Hutten, P. F., Eds.; Wiley-VCH: Weinheim, Germany, 2000.
(18) Brabec, C. J.; Padinger, F.; Hummelen, J. C.; Janssen, R. A. J.; Sariciftci, N. S. *Synth. Met.* **1999**, *102*, 861−864.
(19) Friend, R. H.; Gymer, R. W.; Holmes, A. B.; Burroughes, J. H.; Marks, R. N.; Taliani, C.; Bradley, D. D. C.; Dos Santos, D. A.; Brédas, J. L.; Lögdlund, M.; Salaneck, W. R. *Nature* **1999**, *397*, 121−128.
(20) Tessler, N. *Adv. Mater.* **1999**, *11*, 363−370.
(21) Segura, J. L. *Acta Polym.* **1998**, *49*, 319−344.
(22) Hadziioannou, G.; van Hutten, P. F.; Malliaras, G. G. *Macromol. Symp.* **1997**, *121*, 27−34.
(23) Echegoyen, L.; Echegoyen, L. E. *Acc. Chem. Res.* **1998**, *31*, 593−601.
(24) Geckeler, K. E.; Samal, S. *Polym. Int.* **1999**, *48*, 743−757.
(25) Chen, Y.; Huang, Z.-E.; Cai, R.-F.; Yu, B.-C. *Eur. Polym. J.* **1998**, *34*, 137−151.
(26) Cao, T.; Webber, S. E. *Macromolecules* **1995**, *28*, 3741−3743.
(27) Ederlé, Y.; Mathis, C. *Macromol. Rapid Commun.* **1998**, *19*, 543−547.
(28) Gügel, A.; Belik, P.; Walter, M.; Kraus, A.; Harth, E.; Wagner, M.; Spickermann, J.; Müllen, K. *Tetrahedron* **1996**, *52*, 5007−5014.
(29) Kraus, A.; Müllen, K. *Macromolecules* **1999**, *32*, 4214−4219.
(30) Zhang, N.; Schricker, S. R.; Wudl, F.; Prato, M.; Maggini, M.; Scorrano, G. *Chem. Mater.* **1995**, *7*, 441−442.
(31) Shi, S.; Khemani, K. C.; Li, Q.; Wudl, F. *J. Am. Chem. Soc.* **1992**, *114*, 10656−10657.
(32) Geckeler, K. E.; Hirsch, A. *J. Am. Chem. Soc.* **1993**, *115*, 3850−3851.
(33) Hawker, C. J. *Macromolecules* **1994**, *27*, 4836−4837.
(34) Okamura, H.; Terauchi, T.; Minoda, M.; Fukuda, T.; Komatsu, K. *Macromolecules* **1997**, *30*, 5279−5284.
(35) Szwarc, M. *J. Polym. Sci., Part A: Polym. Chem.* **1998**, *36*, ix-xv.
(36) Dasgupta, A.; Sivaram, S. *J. Macromol. Sci., Rev. Macromol. Chem. Phys.* **1997**, *C37*, 1−59.
(37) Baumert, M.; Frey, H.; Hölderle, M.; Kressler, J.; Sernetz, F. G.; Mülhaupt, R. *Macromol. Symp.* **1997**, *121*, 53−74.
(38) Malmström, E. E.; Hawker, C. J. *Macromol. Chem. Phys.* **1998**, *199*, 923−935.
(39) Hawker, C. J. *Acc. Chem. Res.* **1997**, *30*, 373−382.
(40) Patten, T. E.; Matyjaszewski, K. *Adv. Mater.* **1998**, *10*, 901−915.

In the next section of this paper, we first describe our results on the $C_{60}$ functionalization of styrene-type copolymers via ATRA.[41] A sufficient degree of functionalization should be achieved for $C_{60}$ to form a continuous path for electrons. The second part will deal with the functionalization of a PPV block with an alkoxyamine initiator and its use in the synthesis of rod−coil block copolymers. The controlled radical polymerization of the coil (polystyrene) block leaves the PPV moiety untouched. Finally, the combination of the two approaches into the synthesis of a bifunctional diblock copolymer is demonstrated, and a preliminary photophysical evaluation of this copolymer is presented.

## Results and Discussion

**Functionalization of Random Copolymers with $C_{60}$.** The attachment of styrene to $C_{60}$ by means of radical addition has already been demonstrated by Okamura et al.,[34] using thermally created radicals from alkoxyamine-terminated polymer chains as the radical source. In this method, each $C_{60}$ molecule ends up carrying two polystyrene chains. Since, in Okamura's compounds, the molar ratio of polystyrene to $C_{60}$ is fixed at 2:1, the molecular weights of the polystyrene chains must be below 2000 for the percolation limit of 16 wt % to be attainable, which is required for a continuous conductive path through $C_{60}$. This is one serious drawback of this approach. Furthermore, nonfunctionalized homopolymer may be formed by the recombination of two polystyrene chains during the functionalization step, which complicates workup procedures.

To incorporate more $C_{60}$, multifunctional chains would be advantageous. Instead of the "head-on" attachment used by Okamura et al.,[34] we have aimed at attaching $C_{60}$ as side groups, creating a "charm-bracelet"-type of polymer. We have chosen to employ ATRA of $C_{60}$ to poly(4-chloromethylstyrene) (PCMS), since this polymer has already been used successfully as an initiator for ATRP.[42] However, the presence of two multifunctional components (PCMS and $C_{60}$) makes the occurrence of cross-linking very likely. This was confirmed by experiments using PCMS and different amounts of $C_{60}$; only insoluble products were obtained. We therefore synthesized a series of statistical copolymers of styrene and 4-chloromethylstyrene (CMS), thus diluting the reactive groups with unreactive styrene moieties that act as spacers. The goal was to determine the maximum amount of chloromethyl groups in a random copolymer which still yields soluble functionalized materials.

Random copolymers with different ratios of styrene to CMS ($n = 1, 3, 5$, with $m = 1$, $x$ being in the range 10−20) were synthesized using NMRP with 2,2,6,6-tetramethylpiperidine-1-oxyl (TEMPO) according to Scheme 1. Molecular weights amounted to between $7 \times 10^3$ and $11 \times 10^3$ g/mol with polydispersities ranging from 1.12 to 1.22. These polymers were subsequently functionalized with $C_{60}$. (The nomenclature used throughout the paper uses "Cl" for the chloromethyl-containing polymers and "Fu" for the ones carrying $C_{60}$, followed by the feed ratio of styrene to chloromethylstyrene used in the polymerization.) The composition of the random copolymers as indicated by $^1$H NMR corresponded quite well to the feed ratio. However, no significant difference in chemical shift is observed when $-CH_2-Cl$ is converted to $-CH_2-C_{60}$, ruling out the determination of the degree of functionalization through integration of the corresponding signals.

**Scheme 1.** Synthesis of Statistical Copolymers of Styrene and 4-Chloromethylstyrene and Their Subsequent Functionalization with $C_{60}$

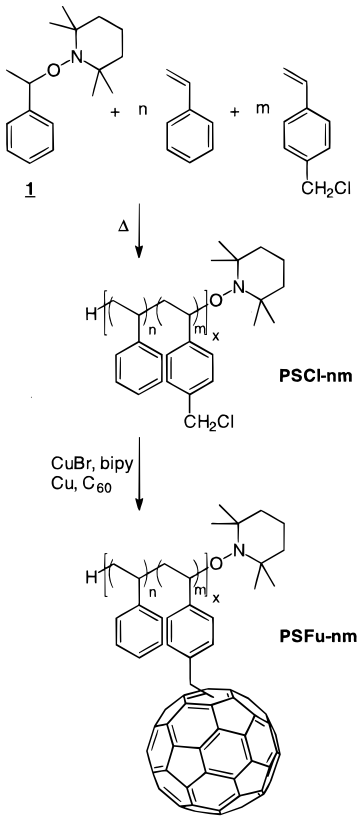


With increasing amounts of chloromethyl groups, the average distance between these groups decreases, and hence the possibility of multiple intramolecular additions on $C_{60}$ will rise. An increase of the concentration of reactive sites on the starting polymer, therefore, may not increase the amount of $C_{60}$ in the resulting polymer. Obviously, an optimization of all reaction parameters is necessary, but this is rather difficult as the determination of the amounts of $C_{60}$ and the number of intra- and intermolecular cross-links is not straightforward.[43]

UV−vis spectrometry might be a convenient method to determine the amount of $C_{60}$ in a copolymer. For this method to be quantitative, values of the molar extinction coefficient are required. However, the fine structures of the absorption spectra of well-defined derivatives of $C_{60}$ (and hence their absorption coefficients at a given wavelength) were shown to be dependent on the substitution pattern as well as on the number of substituents.[44] The randomness in our copolymer will therefore render this method somewhat inaccurate. Still, the absorption spectra can be used to give a qualitative picture of the degree of functionalization. Figure 2 shows the absorption spectra of several copolymers in $CHCl_3$. The top figure depicts the

(41) Iqbal, J.; Bhatia, B.; Nayyar, N. K. *Chem. Rev.* **1994**, *94*, 519−564.

(42) Gaynor, S. G.; Edelman, S.; Matyjaszewski, K. *Macromolecules* **1996**, *29*, 1079−1081.

(43) Elemental analysis was not used as a method for determining the degree of functionalization because of uncertainties concerning the mechanism involved. The radical attachment via TEMPO-functionalized polystyrenes, which yields an unstable fullerene radical−TEMPO adduct after the first addition, leads to the addition of a second radical to form a stable species. Under the ATRA mechanism, the product of the first addition would be an alkylated halogen−fullerene. As $C_{60}$ itself can form stable halogen adducts (see: Hirsch, A. *Synthesis* **1995**, 895−913), the stability of this first adduct cannot be easily predicted. The same is true for the reactivity of this halogenated fullerene toward the ATRA cycle. In the case of a stable halogenated fullerene, the determination of the residual halogen content by means of elemental analysis will not help in estimating the conversion.

(44) Djojo, F.; Herzog, A.; Lamparth, I.; Hampel, F.; Hirsch, A. *Chem. Eur. J.* **1996**, *2*, 1537−1547.

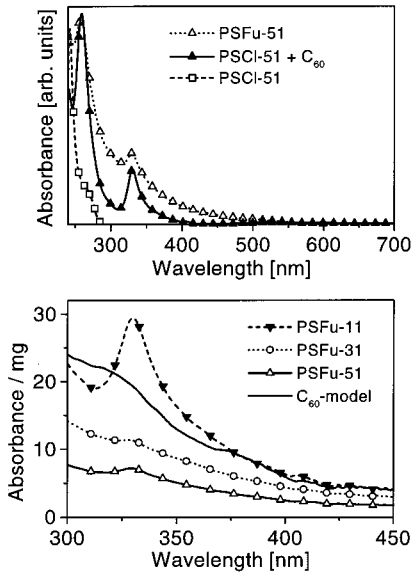


**Figure 2.** Absorption spectra of the copolymers in $CHCl_3$. Top: comparison between solutions of a starting copolymer (PSCl-51) and its $C_{60}$-functionalized form (PSFu-51), and a mixed solution of the starting copolymer and $C_{60}$. Bottom: spectra of solutions of $C_{60}$-functionalized copolymers and of $C_{60}$-model, normalized per milligram of substance.

absorption spectra of the solution of an unfunctionalized copolymer, of a mixed solution of this copolymer and $C_{60}$, and of the solution of the corresponding functionalized copolymer. While the starting material shows no absorption beyond 300 nm, the functionalized copolymer exhibits the bands around 330 nm as well as the long tailing into the visible part of the spectrum that are characteristic for $C_{60}$ (both features also appear in the spectrum of the mixture). Since we found our functionalized copolymer to be soluble in THF while $C_{60}$ is not,[45] absorption in this case cannot be due to adsorbed $C_{60}$.

An evaluation, in Figure 2 (bottom), of the weight-normalized absorption curves shows that the peak around 330 nm grows with increasing amount of chloromethyl groups in the starting copolymers. The spectrum of a substituted fullerene derivative of known $C_{60}$ content ($C_{122}H_{88}O_{15}$, $[C_{60}] = 40$ wt %),[46] to be referred to as $C_{60}$-model in the following, is also shown, allowing an estimation of the $C_{60}$ contents of the polymers. For comparison, an adduct of poly(4-acetoxystyrene) onto $C_{60}$, $(PAcSt)_2$-$C_{60}$, was synthesized according to the method of Okamura et al.[34] The arms of this adduct have a molecular mass of around 2300 g/mol. Its absorption spectrum showed features similar to those of our PSFu copolymers.

If the absorption at 330 nm of $C_{60}$-model is taken as a reference, PSFu-51, PSFu-31, and PSFu-11 would contain 15, 23, and 61 wt % $C_{60}$, respectively. A value of 13 wt % is found for $(PAcSt)_2$-$C_{60}$, which agrees well with that calculated from its composition. The $C_{60}$ content of this compound is low despite the low molecular weight of its arms, because it is obtained via addition to the chain end. Our approach, using addition to side groups, has obvious advantages in this respect.

The different shape of the absorption band of $C_{60}$-model indicates that the values obtained through normalization of the absorption spectra and comparison to this model compound can only be a crude estimate. On the other hand, the agreement found for $(PAcSt)_2$-$C_{60}$ indicates that the method may be used with some confidence for the determination of the $C_{60}$ content.

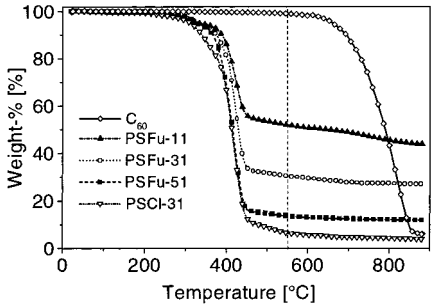


**Figure 3.** TGA of several copolymers and of $C_{60}$ under $N_2$. Heating rate 10 °C/min.

**Table 1.** Results of TGA and Absorption Spectroscopy for $C_{60}$-Functionalized Copolymers, $C_{60}$, and Derivatives Thereof

| sample | TGA residue at 550 °C (wt %) | relative absorbance at 330 nm[a] |
|---|---|---|
| PSFu-51 | 14 | 15 |
| PSFu-31 | 31 | 23 |
| PSFu-11 | 52 | 61 |
| $(PAcSt)_2-C_{60}$ | 21 | 13 |
| $C_{60}$ | 99 | |
| $C_{60}$-model | 49 | 40 |

[a] Values are normalized with respect to the value of 40 for $C_{60}$-model, which corresponds to its $C_{60}$ content.

Alternatively, the $C_{60}$ content may be determined by means of thermogravimetric analysis (TGA). Figure 3 shows the results for one of the starting polymers, for the $C_{60}$-functionalized polymers as well as for pure $C_{60}$. Whereas the latter is stable up to 550 °C, the polymers start to decompose at much lower temperatures. Since this decomposition is almost complete at 550 °C, it is safe to assume that the residue at this temperature corresponds to the $C_{60}$ content. Clearly then, TGA shows that the amount of $C_{60}$ increases with the fraction of chloromethyl groups in the starting material.

Table 1 summarizes the results from TGA and UV. Although the absolute values obtained differ, the overall trend of increasing $C_{60}$ content with increasing number of chloromethyl groups is confirmed. The higher value for $(PAcSt)_2$-$C_{60}$ obtained from the TGA may be related to cross-linking of the poly(4-acetoxystyrene) upon heating, resulting in a larger residue at 550 °C. The same seems to be the case for $C_{60}$-model, again indicating that also TGA does not give absolute values.

To test whether there is unreacted polymer in the functionalized samples, GPC elugrams were taken in THF with UV detection. Figure 4 shows the comparison between PSCl-51 and PSCl-31 together with the corresponding $C_{60}$-functionalized copolymers. Copolymer PSFu-11 was not sufficiently soluble in THF to be included in this series of experiments.

The insets of Figure 4 show the refractive index GPC elugrams obtained. For the starting materials, they are very narrow, as expected for NMRP. After functionalization, the GPC traces are broader and show additional features. The main graphs show the absorption spectra of starting and functionalized material. Note the absence of absorption by the starting material PSCl in this wavelength range. The spectra show, however, that for each of the different positions in the elugram of the functionalized material, absorption at 330 nm occurs. From this we conclude that the functionalization via ATRA proceeds very smoothly and effectively. A sizable absorption is also found for retention times within the range covered by the elugram of the unfunctionalized starting material. In the case of PSFu-51,

(45) Ruoff, R. S.; Tse, D. S.; Malhotra, R.; Lorents, D. C. *J. Phys. Chem.* **1993**, *97*, 3379−3383.
(46) Nierengarten, J.-F.; Felder, D.; Nicoud, J.-F. *Tetrahedron Lett.* **1999**, *40*, 273−276.

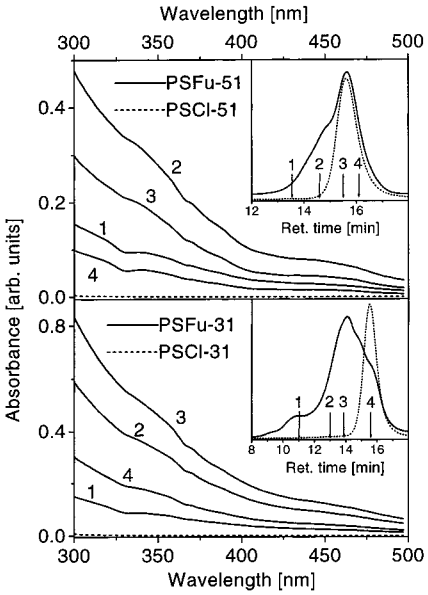


**Figure 4.** GPC elugrams (insets) and absorption spectra of starting (- - -) and $C_{60}$-functionalized (—) copolymers in THF. Absorption spectra 1−4 of the $C_{60}$ copolymers correspond to different positions in the elugrams as indicated in the insets.

the maximum of the elugram is not shifted relative to that of the starting material. This implies that the hydrodynamic volume of the chains in this fraction has not changed significantly upon incorporation of $C_{60}$, suggesting, rather, that binding a $C_{60}$ molecule somehow results in a contractile effect opposing excluded-volume interactions. Intramolecular cross-linking may be involved. A similar conclusion holds for the more densely substituted copolymer, although the maxima of the elugrams are at different positions. There is a shoulder in the elugram of PSFu-31 at the position of the maximum found for PSCl-31, and the right-hand edges of the elugrams coincide. The additional details visible in the elugrams suggest the presence of larger entities comprising a (limited) number of chains. Interchain cross-linking due to the high volume density of functional groups is probably involved in the formation of these entities.

In conclusion, the controlled incorporation of $C_{60}$ into copolymers of styrene and 4-chloromethylstyrene by means of atom transfer radical addition to the fullerene is feasible. While the amount of $C_{60}$ incorporated into the copolymer can be predetermined to a certain extent via the feed ratio of styrene to chloromethylstyrene, the length of the copolymer itself is controlled by the use of nitroxide-mediated free radical polymerization. Other methods to incorporate fullerenes into copolymers shown so far in the literature (azide, cycloaddition, esterification) include multiple synthetic steps to obtain the functional monomers/prepolymers, whereas our approach involves only two steps (polymerization, ATRA) with commercially available compounds. These features make our approach attractive for the synthesis of block copolymers in which one block contains the $C_{60}$ functionalization.

**Synthesis of Rod−Coil Block Copolymers Based on PPV as the Rigid Rod.** Most of the rod−coil block copolymers with conjugated polymers or oligomers as the rigid rod synthesized so far[47−54] were obtained by anionic polymerization of the coil polymer, followed by quenching, either with a reactive end group on the rigid conjugated block or with a functional molecule to obtain an end-functionalized coil polymer that is subsequently coupled to the conjugated block. Jenekhe et al.[48] synthesized block copolymers in which the conjugated block was made through a polycondensation from a functionalized polystyrene block. These strategies have some drawbacks, however. When a coupling reaction is performed between two polymer blocks, one block is usually present in large excess to drive the reaction to completion. This necessitates tedious workup procedures to ensure removal of the unreacted homopolymer. The quenching of an anionic polymerization with a functional conjugated block can yield dead homopolymer if contaminants that act as a quencher, such as water or solvent, are introduced with the addition of the rigid rod part. Hence, tedious workup procedures can only be avoided at the cost of an elaborate preparation of the starting materials. Furthermore, as anionic polymerizations have to be carried out in closed systems, the synthesis of a series of block copolymers with varying block lengths is a very laborious task. Conjugated polymers, on the other hand, are mostly synthesized by polycondensation reactions. Since polycondensations do not require initiation, growth from a specific site is highly unlikely, if not impossible. Furthermore, the use of an end-capping reagent, as demonstrated by Jenekhe et al.,[48] would require 100% conversion of the polycondensation to circumvent the presence of homopolymer, unless the end cap is much more reactive than the other reactive groups. Otherwise, large amounts of homopolymer have to be removed during workup. Overall, this is not a very convenient method for the synthesis of block copolymers with a conjugated rod block.

The use of anionic polymerization techniques to obtain rod−coil block copolymers was demonstrated by Leclère et al.[52] It employs an anionically polymerized precursor of the conjugated block that is subsequently converted into its conjugated form in a polymer-analogous reaction after the incorporation of the second (coil) block. While this method truly employs living polymerization techniques, it suffers from the necessity of a second, polymer-analogous reaction step, where failure to achieve full conversion leads to permanent defects in the conjugated block. These defects might be detrimental in photonic applications of the polymer.

A completely different and more versatile approach to the synthesis of (conjugated) rod−coil block copolymers is the use of an initiator for living polymerization that is attached to the rigid block. The living nature of the polymerization brings clear advantages. It enables one to synthesize a series of polymers with varying block ratios from one batch. Each polymerization would start from the same conjugated block, which makes the comparison of different samples more straightforward. Moreover, this method allows the full characterization and purification of the conjugated block before its functionalization. For the attachment of the initiator onto the conjugated block, a huge excess of initiator can be used to ensure full conversion. The unreacted molecules can be simply removed by precipitation

(47) Li, W.; Wang, H.; Yu, L.; Morkved, T. L.; Jaeger, H. M. *Macromolecules* **1999**, *32*, 3034−3044.
(48) Jenekhe, S. A.; Chen, X. L. *Science* **1998**, *279*, 1903−1907.
(49) Kukula, H.; Ziener, U.; Schöps, M.; Godt, A. *Macromolecules* **1998**, *31*, 5160−5163.
(50) Marsitzky, D.; Brand, T.; Geerts, Y.; Klapper, M.; Müllen, K. *Macromol. Rapid Commun.* **1998**, *19*, 385−389.
(51) Hempenius, M. A.; Langeveld-Voss, B. M. W.; van Haare, J. A. E. H.; Janssen, R. A. J.; Sheiko, S. S.; Spatz, J. P.; Möller, M.; Meijer, E. W. *J. Am. Chem. Soc.* **1998**, *120*, 2798−2804.
(52) Leclère, Ph.; Parente, V.; Brédas, J. L.; François, B.; Lazzaroni, R. *Chem. Mater.* **1998**, *10*, 4010−4014.
(53) Tew, G. N.; Pralle, M. U.; Stupp, S. I. *J. Am. Chem. Soc.* **1999**, *121*, 9852−9866.
(54) Marsitzky, D.; Klapper, M.; Müllen, K. *Macromolecules* **1999**, *32*, 8685−8688.

**Scheme 2.** Synthesis of the Alkoxyamine Initiator, the Aldehyde-Functionalized PPV Block, and Their Combination into the Macroinitiator

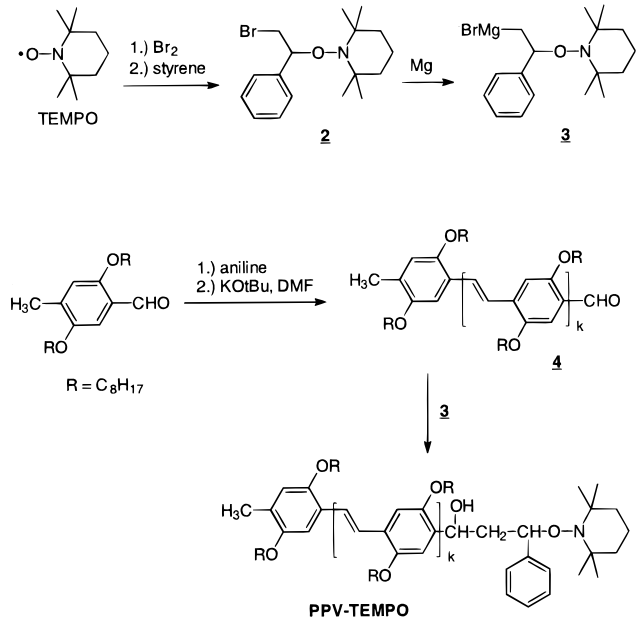


of the polymer, once more yielding a well-defined starting system. Marsitzky et al.[54] demonstrated this approach recently, anionically grafting ethylene oxide from a polyfluorene block.

We chose NMRP as the controlled/"living" polymerization method, for several reasons. Radical polymerization itself tolerates a number of functional groups and does not require stringent starting material purification. It does not interfere with either the olefinic double bonds of the PPV part or the substituents on the rings. The synthesis of the monofunctionalized PPV block, as well as the attachment of the initiator, is outlined in Scheme 2. A similar methodology, yielding ABA block copolymers in a one-pot synthesis, was recently introduced by Klaerner et al.[55]

Poly(2,5-dioctyloxy-1,4-phenylenevinylene) was selected as the rigid part of our block copolymers. The synthesis was carried out via the Siegrist polycondensation as originally described by Kretzschmann et al.[56,57] By this method, which uses the condensation of para-substituted methylbenzaldimines under strong basic conditions as depicted in Scheme 2, oligo(phenylenevinylene)s of narrow chain length distribution[57] that carry exactly one terminal aldehyde group per molecule are obtained. This is essential for the subsequent functionalization. Control of chain length can be exercised by varying the reaction temperature. At room temperature, the oligomers precipitate already after an average of four addition steps. Temperatures around 80 °C, on the other hand, may result in oligomer mixtures that reach or exceed the effective conjugation length of 12 repeating units.[58] A further advantage is the fact that this method yields only oligomers with *trans*-configured vinylic double bonds,[59] rendering the conjugated block virtually defect-free.

The attachment of the initiator to the rigid PPV block occurs via the nucleophilic attack of a Grignard reagent to the aldehyde group. An excess of the Grignard reagent guarantees complete functionalization, as shown by the disappearance of the aldehyde signal in $^1$H NMR, while the solubility of the initiator facilitates subsequent purification of the resulting PPV−initiator compound. The alkoxyamine initiator containing a bromide group for the formation of the Grignard reagent can be easily obtained by the reaction of TEMPO with $Br_2$, followed by the addition of styrene, as described by Kobatake et al.[60] and shown in the upper part of Scheme 2. The lower part of this scheme depicts the synthesis of the TEMPO-functionalized PPV block via Grignard addition.

The average degree of polymerization of the PPV block can be determined either by end-group analysis with $^1$H NMR or by UV−vis spectroscopy. As $^1$H NMR relies on the comparison of huge and small signals, it loses its accuracy with increasing molecular weight or when signals overlap. Therefore, we used the combination of both methods. For the end-group analysis, the peaks of the methyl end group at 2.2 ppm and the signals for the $OCH_2$ groups at 4.0 ppm were used. An average degree of polymerization of 10 repeat units was calculated by this method for the macroinitiator PPV-TEMPO. The UV−vis spectrum, on the other hand, shows a maximum absorption at 467 nm, which corresponds to seven phenylenevinylene repeat units.[58] The comparison with the absorption spectrum of the seven-ring oligomer of ref 58 indicates the presence of higher oligomers in our PPV material. This is also corroborated by GPC using UV detection. The too high value obtained from $^1$H NMR is attributed to the inaccuracy of the method. The calculations of molecular weights presented later in the paper are based on a value of seven repeat units ($M_n = 2.5 \times 10^3$ g/mol) for the PPV part.

The TEMPO-functionalized PPV block is subsequently used as a macroinitiator in NMRP of styrene, as depicted in Scheme 3 (top). Samples of the PPV-*b*-PS system were taken after time intervals of 50, 95, and 105 min to investigate its living character. $^1$H NMR was used for molecular weight determination. The technique is used here only to find the weight ratio between the PPV and PS blocks, for which it is an accurate procedure.

The values in Table 2 indicate that the PS block grows steadily with reaction time. The trend is obvious and shows that polymerization of styrene with a macroinitiator is feasible. While GPC experiments also indicated an increase in molecular weight with conversion, those results cannot be used as absolute values due to the lack of appropriate standards for calibration.

**Synthesis and Photophysical Properties of PPV−$C_{60}$-Functionalized PS Diblock Copolymers.** With the objective of bringing PPV and $C_{60}$ together in one molecule, we combined the results of the two previous sections into the synthesis of a random copolymer of styrene and CMS from our PPV-based macroinitiator (Scheme 3, bottom). A feed ratio of styrene to CMS of 2:1 was chosen to ensure solubility of the $C_{60}$-containing material. $^1$H NMR analysis of the block copolymer indicated that the actual ratio of styrene to CMS is 1.5, and that the molecular weight of the styrenic block is $9 \times 10^3$ g/mol.

Subsequently, this block copolymer was functionalized with $C_{60}$. Figure 5 shows UV spectra and TGA of the starting PPV-*b*-poly(styrene-*stat*-CMS) and the $C_{60}$-containing block copolymer. The increase in residue at 550 °C from 14 to 60 wt % upon functionalization of the rod−coil block copolymer with

(55) Klaerner, G.; Trollsås, M.; Heise, A.; Husemann, M.; Atthoff, B.; Hawker, C. J.; Hedrick, J. L.; Miller, R. D. *Macromolecules* **1999**, *32*, 8227−8229.

(56) Kretzschmann, H.; Meier, H. *Tetrahedron Lett.* **1991**, *32*, 5059−5062.

(57) Kretzschmann, H.; Meier, H. *J. Prakt. Chem.* **1994**, *336*, 247−254.

(58) Meier, H.; Stalmach, U.; Kolshorn, H. *Acta Polym.* **1997**, *48*, 379−384.

(59) Meier, H. *Angew. Chem.* **1992**, *104*, 1425−1446. Meier, H. *Angew. Chem., Int. Ed. Engl.* **1992**, *31*, 1399−1420.

(60) Kobatake, S.; Harwood: H. J.; Quirk, R. P.; Priddy, D. B. *Macromolecules* **1999**, *32*, 10−13.

**Scheme 3.** Block Copolymer Synthesis Using the PPV−TEMPO Macroinitiator for NMRP

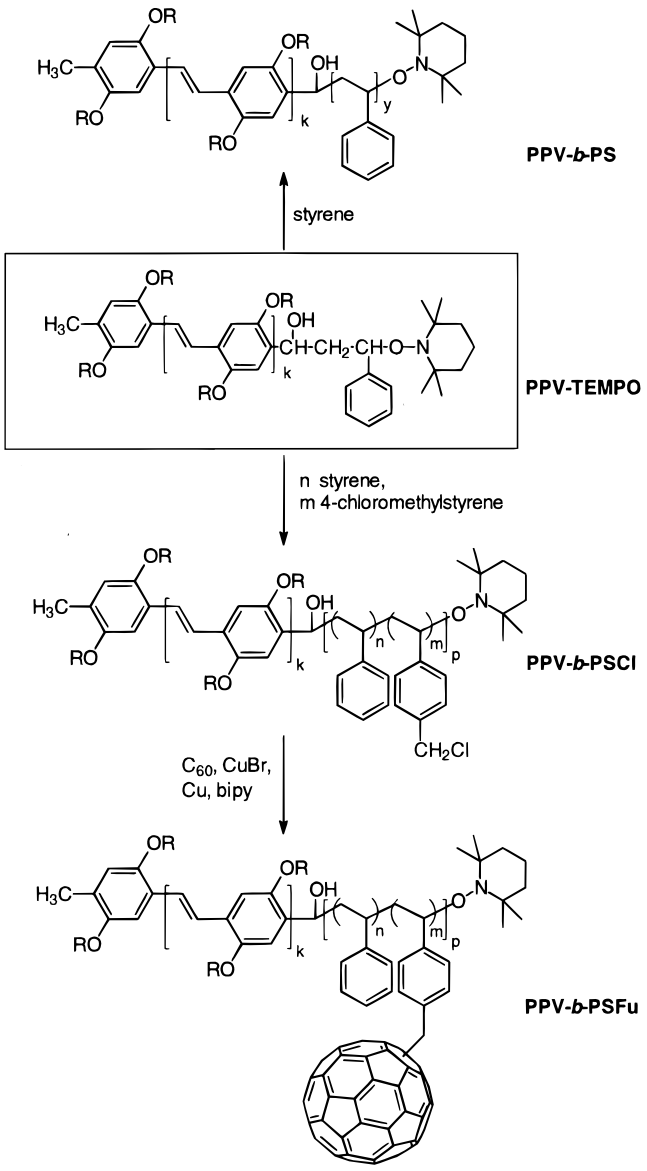


**Table 2.** Composition (Weight Ratio) and Molecular Weight of PPV−Polystyrene Diblock Copolymers As Determined via $^1$H NMR on Solutions in Chloroform ($M_{N,PPV} = 2.5 \times 10^3$ g/mol)

| sample | $w_{PS}$:$w_{PPV}$ | $M_n$ ($10^3$ g/mol) |
|---|---|---|
| PPV-*b*-PS(50) | 0.4 | 3.6 |
| PPV-*b*-PS(95) | 1.5 | 6.3 |
| PPV-*b*-PS(105) | 1.8 | 7.0 |

$C_{60}$ is very well visible in the TGA graph of Figure 5 (top). This indicates an average of around 15 fullerene molecules per chain, and translates into one $C_{60}$ for every two reactive sites in the starting polymer. In the bottom part of Figure 5, weight-normalized absorption spectra are shown. The absorption band of the PPV block is centered around 465 nm. A comparison with the spectrum of the PPV macroinitiator suggests the weight ratio of the PS block to the PPV block to be around 3. The $C_{60}$ functionalization by means of ATRA little affects the absorption band of the PPV block, indicating that the conjugated block remains intact. When $C_{60}$-model is again used as the reference for a spectroscopic determination of the $C_{60}$ content of PPV-*b*-PSFu, based on the weight-normalized value of the absorbance at 330 nm, the result agrees well with the TGA result.

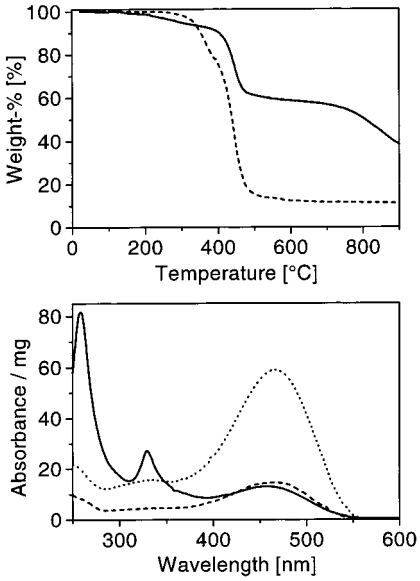


**Figure 5.** Comparison of the starting diblock copolymer PPV-*b*-PSCl (- - -) and the $C_{60}$-functionalized diblock copolymer PPV-*b*-PSFu (—). Top: TGA, heating rate 10 °C/min. Bottom: absorption spectra in $CHCl_3$; the spectrum of the PPV−TEMPO macroinitiator is shown for comparison (•••).

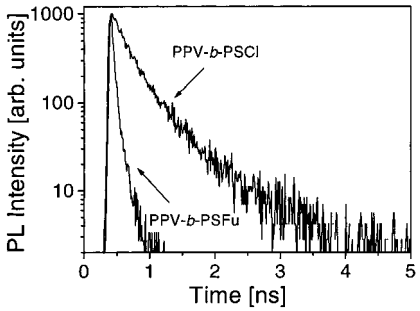


**Figure 6.** Photoluminescence decay curves of spin-cast films of the rod−coil diblock copolymer PPV-*b*-PSCl and its functionalized derivative, the donor−acceptor diblock PPV-*b*-PSFu.

The suitability of the type of block copolymer described above for application in photovoltaic devices relies, among other things, on the abilities of the respective blocks to function as electron donor and acceptor, and as charge transport media. As outlined in the Introduction, the microstructure is a crucial factor to both these functions. The efficiency of the electron transfer between the excited donor (PPV) and the acceptor ($C_{60}$) may be assessed from the extent to which luminescence from the donor block is suppressed ("quenched"). Figure 6 shows luminescence decay curves of spin-cast thin films of our block copolymers, both the rod−coil diblock (PPV-*b*-PSCl) and its $C_{60}$-functionalized form (PPV-*b*-PSFu). While the former has a dominant photoluminescence decay time of around 250 ps, the decay time found for the donor−acceptor block copolymer is equal to or below the instrumental response time of about 50 ps. The quenching indicates that electron transfer from an excited PPV block to a $C_{60}$ substituent of the PS block occurs efficiently. This result is a very preliminary one, since no control whatsoever has been exerted over the microstructure. It is a promising starting point for further studies dealing with its optimization.

**Micrometer-Scale Pattern Formation in Diblock Copolymers.** Upon casting films from $CS_2$ solution (a selective solvent for PS), the formation of honeycomb patterns on a micrometer scale was observed, for the PPV-*b*-PS copolymer as well as for

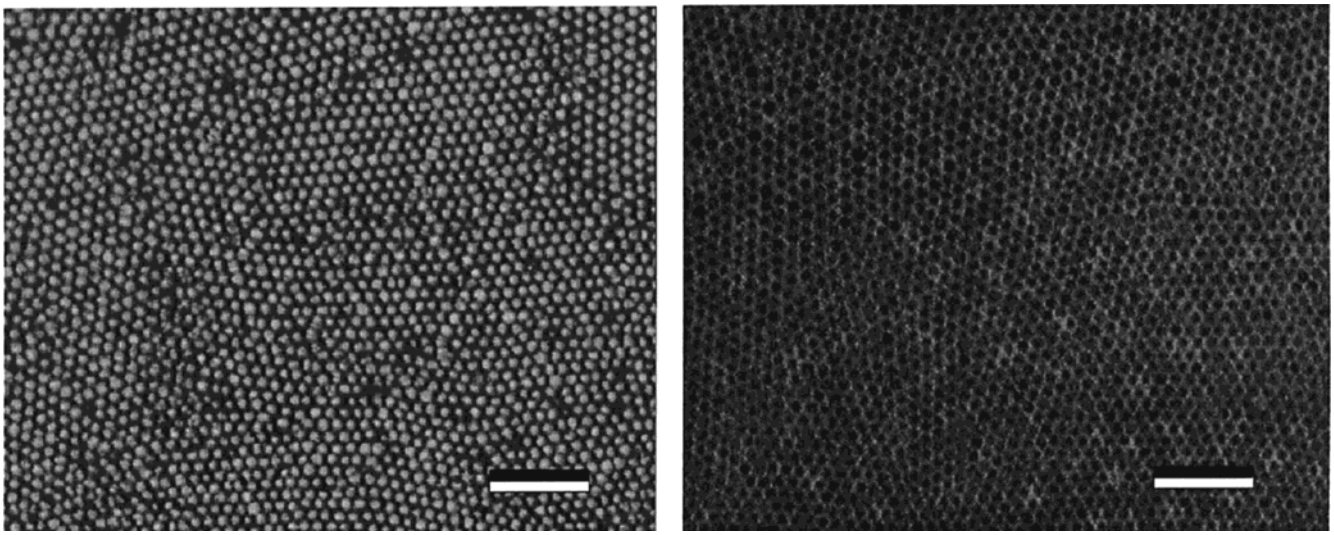

**Figure 7.** Optical transmission (left) and luminescence (right) micrographs of honeycomb structures in solution-cast films of PPV-*b*-PSFu. Due to strong quenching of the luminescence from PPV by $C_{60}$ in the diblock copolymer, the intensity was found to be reduced by 3 orders of magnitude relative to that from a PPV-*b*-PS honeycomb. Scale bars: 20 $\mu$m.

PPV-*b*-PSFu (Figure 7). The sizes of the holes and their spacing are a few micrometers, 3 orders of magnitude higher than the characteristic size of the macromolecules and that of the mesophases in common microphase-separated block copolymers! Moreover, hole formation is not observed in block copolymer microphase separation. Clearly, other physical phenomena are at play here. Similar hexagonal patterns have been previously observed and studied in detail in thin liquid layers that have a free upper surface and are heated from below.[61] In the polymer field, this phenomenon has been reported by François and co-workers[62,63] for poly(*p*-phenylene)−polystyrene block copolymers and by Jenekhe and Chen[64] for poly(phenylquinoline)−polystyrene, among others. Whereas honeycomb material obtained from PPV-*b*-PS shows a strong yellow-orange luminescence, the luminescence intensity is very low in PPV-*b*-PSFu. Luminescence is quenched to such an extent by the $C_{60}$ side groups that, to obtain images of similar brightness, an exposure time approximately 1000 times as long as that for PPV-*b*-PS is necessary for PPV-*b*-PSFu.

The structure formation discussed here may be useful for obtaining optical band gap materials or patterned LEDs, for instance. A fundamental understanding of the physicochemical principles underlying the pattern formation is still lacking and urgently needed for engineering and controlled fabrication.

## Conclusion

We demonstrated the successful synthesis of rod−coil block copolymers containing a PPV block as the rigid part and a flexible PS coil obtained by means of nitroxide-mediated "living" radical polymerization. For this, a macroinitiator was prepared by covalently connecting the PPV block to an alkoxyamine derived from TEMPO. Polymerization of styrene from this PPV block proceeds with a steady increase of the PS block length with reaction time. Following the same approach and starting from the same PPV block as the donor part, we also successfully synthesized a donor−acceptor diblock copolymer for use in photovoltaic devices. Atom-transfer radical addition to a chloromethyl group was used to graft $C_{60}$ (acceptor) onto the flexible part of the block copolymer, which consisted of a random copolymer of styrene and 4-chloromethylstyrene in this case. The conditions for maximum functionalization with $C_{60}$ by this method were explored with the help of several random copolymers of styrene and chloromethylstyrene synthesized via nitroxide-mediated living radical polymerization. An increased feed ratio of chloromethylstyrene to styrene led to a higher $C_{60}$ content of the copolymers. However, this also gave rise to increased cross-linking, resulting in less soluble products. Efficient electron transfer at the donor−acceptor interface was confirmed by the quenching of the luminescence from the PPV block. Films obtained through a casting process from $CS_2$ exhibit honeycomb structuring at the micrometer level, a feature which opens up new possibilities for photonic applications.

## Experimental Section

**Materials and Methods.** THF was distilled from Na/K alloy, ether from $LiAlH_4$, and toluene from Na/benzophenone. Chemicals were used as received, unless noted otherwise. The unimolecular TEMPO initiators **1** and **2** were synthesized according to refs 65 and ref 60, respectively.

NMR spectra were recorded on a Varian Gemini-300 spectrometer with internal lock on the $^2H$ signal of the solvent. Absorbance spectra were measured with a SLM Aminco 3000 diode array spectrometer. Thermogravimetric analyses were carried out with a Perkin-Elmer TGA7 at a heating rate of 10 °C/min under a nitrogen atmosphere. The GPC measurements were done in THF using PL-gel mixed-C columns in a Waters Powerline 600 LC-system, equipped with a Waters 996 photodiode detector and a Wyatt Dawn DSP light-scattering detector. Luminescence lifetime measurements were made with a Hamamatsu C5680 streak camera attached to a Chromex 0.25 m spectrograph, and using the second harmonic of a Ti:sapphire laser equipped with a pulse picker for excitation ($\lambda$ = 446 nm).

**Copolymerization.** Random copolymers were prepared by mixing appropriate amounts of monomer with **1**. After addition of a small amount of acetic anhydride, the mixtures were degassed by several freeze−pump−thaw cycles, flushed with dry nitrogen, and subsequently immersed in an oil bath kept at 135 °C for 5 h, when the reaction mixture solidified. After being cooled to room temperature, the polymer was dissolved in $CHCl_3$ and precipitated in methanol. The precipitate was filtered, redissolved in $CHCl_3$, and precipitated in methanol again. After filtration, the polymer was dried under vacuum at 50 °C.

(61) Schatz, M. F.; VanHook, S. J.; McCormick, W. D.; Swift, J. B.; Swinney, H. L. *Phys. Rev. Lett.* **1995**, *75*, 1938−1941.
(62) Widawski, G.; Rawiso, M.; François, B. *Nature* **1994**, *369*, 387−389.
(63) Pitois, O.; François, B. *Eur. Phys. J. B* **1999**, *8*, 225−231.
(64) Jenekhe, S. A.; Chen, X. L. *Science* **1999**, *283*, 372−375.
(65) Matyjaszewski, K.; Woodworth, B. E.; Zhang, X.; Gaynor, S. G.; Metzner, Z. *Macromolecules* **1998**, *31*, 5955−5957.

PSCl-11: 0.13 g (0.5 mmol) of **1**, 1.06 g (10.2 mmol) of styrene, 1.10 g (7.2 mmol) of 4-chloromethylstyrene, yield 0.88 g of polymer, $M_n = 6.7 \times 10^3$ g/mol, $M_w = 8.2 \times 10^3$ g/mol, $M_w/M_n = 1.22$.

PSCl-31: 0.13 g (0.5 mmol) of **1**, 2.08 g (20.0 mmol) of styrene, 1.02 g (6.7 mmol) of 4-chloromethylstyrene, yield 2.0 g of polymer, $M_n = 10.6 \times 10^3$ g/mol, $M_w = 12.8 \times 10^3$ g/mol, $M_w/M_n = 1.21$.

PSCl-51: 0.13 g (0.5 mmol) of **1**, 2.08 g (20.0 mmol) of styrene, 0.61 g (4.0 mmol) of 4-chloromethylstyrene, yield 1.66 g of polymer, $M_n = 7.7 \times 10^3$ g/mol, $M_w = 8.6 \times 10^3$ g/mol, $M_w/M_n = 1.12$.

Representative $^1$H NMR (300 MHz, $CDCl_3$) for PSCl-51: $\delta$ (ppm) = 1.39/1.79 (br s, aliphatic CH, $CH_2$), 4.47 (br s, $CH_2Cl$), 6.54/7.03 (br s, aromatic CH).

**Functionalization with $C_{60}$.** The corresponding copolymer was dissolved with $C_{60}$, $Cu^{(0)}$, CuBr, 2,2′-bipyridine (bipy), and toluene, and degassed by evacuation and subsequent flushing with dry $N_2$. The mixture was then refluxed for 6 h. After being cooled to room temperature, the reaction mixture was filtered and the solvent evaporated under vacuum. The residue was taken up in THF and filtered again. The filter was subsequently washed until the filtrate was colorless. The combined organic phases were concentrated under reduced pressure and precipitated into methanol. The thus obtained brown residue was taken up in a small amount of $CHCl_3$, precipitated again in methanol, filtered, and dried at 50 °C under vacuum overnight.

PSFu-11: 0.35 g of PSCl-11, 0.49 g (0.68 mmol) of $C_{60}$, 0.017 g (0.12 mmol) of CuBr, 0.085 g (1.4 mmol) of Cu, 0.14 g (0.9 mmol) of bipy, 150 mL of toluene, yield 0.26 g of polymer.

PSFu-31: 0.47 g of PSCl-31, 0.36 g (0.50 mmol) of $C_{60}$, 0.021 g (0.15 mmol) of CuBr, 0.1 g (1.6 mmol) of Cu, 0.1 g (0.6 mmol) of bipy, 150 mL of toluene, yield 0.3 g of polymer, $M_n = 9.3 \times 10^4$ g/mol, $M_w = 36.9 \times 10^4$ g/mol, $M_w/M_n = 3.98$.

PSFu-51: 0.29 g of PSCl-51, 0.25 g (0.35 mmol) of $C_{60}$, 0.007 g (0.05 mmol) of CuBr, 0.05 g (0.8 mmol) of Cu, 0.1 g (0.6 mmol) of bipy, 150 mL of toluene, yield 0.2 g of polymer, $M_n = 15.8 \times 10^3$ g/mol, $M_w = 34.0 \times 10^3$ g/mol, $M_w/M_n = 2.15$.

Representative $^1$H NMR (300 MHz, $CDCl_3$) for PSFu-51: $\delta$ (ppm) = 1.38/1.78 (br s, aliphatic CH, $CH_2$), 4.46 (br s, $CH_2X$, X = Cl or $C_{60}$), 6.52/7.02 (br s, aromatic CH).

***ω*-Formylpoly(2,5-dioctyloxy-1,4-phenylenevinylene) (4)** was synthesized according to literature procedures[57] at 80 °C for 2 h, starting from 10 g of 2,5-dioctyloxy-*p*-tolylaldehyde. To hydrolyze the aldimine end group, the reaction mixture was cooled and poured into a mixture of 1000 mL of 1 N HCl and 2000 mL of $CHCl_3$. After the mixture was stirred for 20 min, the organic layer was separated and washed with water until the aqueous phase was neutral. The organic phase was dried over $Na_2SO_4$, concentrated, and twice precipitated into a large excess of acetone. The red powder was filtered and dried at 50 °C under vacuum. The $^1$H NMR spectrum corresponded to the literature data.

**PPV−TEMPO.** A solution of the bromosubstituted alkoxyamine **2** (1.2 g, 3.5 mmol) in 10 mL of dry THF was slowly added to 0.16 g (6.6 mmol) of Mg turnings in 30 mL of dry THF. After being stirred for 2 h at room temperature, the resulting solution of the Grignard reagent **3** was added to a solution of PPV−aldehyde **4** (1.5 g) in 400 mL of dry THF kept at 60 °C and stirred overnight. After the reaction mixture was cooled to room temperature, it was poured into a large excess of ethanol that contained a small amount of HCl. The resulting red powder was filtered, dissolved in $CHCl_3$, and precipitated in ethanol again. Drying at 50 °C under vacuum resulted in 1.3 g of the TEMPO-functionalized PPV block: $^1$H NMR (300 MHz, $CDCl_3$) $\delta$ (ppm) = 0.7−1.9 (m, aliphatic $CH_2$, $CH_3$), 2.2 (s, aromatic $CH_3$), 4.0 (s, $OCH_2$), 4.6, 4.7 (2 s, CHOX, X = H, N), 7.1 (br s, aromatic CH), 7.4 (br s, olefinic CH).

**PPV-*b*-PS.** A 0.6 g sample of PPV−TEMPO, 5.5 g (53 mmol) of styrene, and 0.2 g of acetic anhydride were mixed in a vessel, degassed by three freeze−pump−thaw cycles, and immersed into a thermostat oil bath kept at 130 °C. Samples were taken after 50, 95, and 105 min (when the reaction mixture had solidified), diluted with $CHCl_3$, and precipitated twice in methanol.

Representative $^1$H NMR (300 MHz, $CDCl_3$) for PPV-*b*-PS(50): $\delta$ (ppm) = 0.8 (s, aliphatic $CH_3$), 1.3/1.8 (m, aliphatic CH, $CH_2$), 2.2 (br s, aromatic $CH_3$), 4.0 (br s, $OCH_2$), 5.1 (s, CHOX, X = H, N), 6.5/7.0 (br s, aromatic CH), 7.4 (br s, olefinic CH).

**PPV-*b*-PSCl.** A 0.2 g sample of PPV−TEMPO, 0.83 g (8.0 mmol) of styrene, 0.61 g (4.0 mmol) of 4-chloromethylstyrene, and 0.2 g of acetic anhydride were mixed in a vessel, degassed by three freeze−pump−thaw cycles, and immersed into a thermostat oil bath kept at 135 °C. After 2 h, the reaction mixture had solidified. It was diluted with $CHCl_3$ and precipitated twice in methanol. Yield: 0.47 g of a red powder. $^1$H NMR (300 MHz, $CDCl_3$): $\delta$ (ppm) = 0.8 (br s, aliphatic $CH_3$), 1.3/1.8 (m, aliphatic CH, $CH_2$), 2.2 (br s, aromatic $CH_3$), 4.0 (br s, $OCH_2$), 4.5 (br s, $CH_2Cl$), 6.5/7.0 (br s, aromatic CH), 7.4 (br s, olefinic CH).

**PPV-*b*-PSFu.** A 0.1 g sample of PPV-*b*-PSCl, 0.2 g (0.3 mmol) of $C_{60}$, 0.011 g (0.08 mmol) of CuBr, 0.017 g (0.27 mmol) of Cu, and 0.052 g (0.33 mmol) of bipy were dissolved in 30 mL of 1,2-dichlorobenzene and degassed by bubbling dry nitrogen through the solution for 15 min. Then the reaction mixture was heated to 120 °C for 3 h, cooled to room temperature, and filtered. The filter was washed several times with toluene and the solvent subsequently removed under reduced pressure. THF was added to the residue, and the brown solution was filtered. After the filter was washed with THF until the solvent remained colorless, the resulting solution was concentrated and precipitated twice in methanol. This yielded 50 mg of a brown powder. $^1$H NMR (300 MHz, $CDCl_3$): $\delta$ (ppm) = 0.8 (br s, aliphatic $CH_3$), 1.3/1.8 (m, aliphatic CH, $CH_2$), 2.18 (br s, aromatic $CH_3$), 4.00 (br s, $OCH_2$), 4.5 (br s, $CH_2X$, X = Cl or $C_{60}$), 6.5/7.0 (br s, aromatic CH), 7.4 (br s, olefinic CH).

**Acknowledgment.** We thank G. Alberda van Ekenstein and J. Vorenkamp for TGA and GPC measurements, respectively. We also thank Dr. J.-F. Nierengarten (IPCMS-GMO-CNRS, Strasbourg, France) for making the $C_{60}$-model compound available to us. Financial support from NWO, FOM, and the EU (TMR scholarship for U.S.) is gratefully acknowledged.

JA000160A